

Analysis of stochastic torus-type bursting in 3D neuron model

Lev B. Ryashko
lev.ryashko@urfu.ru

Evdokia S. Slepukhina
evdokia.slepukhina@urfu.ru

Ural Federal University (Yekaterinburg, Russia)

Abstract

We study the stochastic dynamics of the Hindmarsh–Rose model of neuronal activity in the parametrical zone close to the Neimark–Sacker bifurcation. We show that in this zone, random disturbances transform the tonic spiking dynamic regime into the bursting one. This stochastic phenomenon is confirmed by the approximations of the probability density functions for the distribution of random trajectories as well as the interspike intervals statistics. For a quantitative analysis of the noise-induced bursting, we suggest and effectively apply a constructive approach based on the stochastic sensitivity function technique and the method of confidence domains.

1 Introduction

As a biological system, a neuron is very sensitive to random disturbances. Therefore, the study of phenomena related to the influence of noise on the neuron models, is of significant interest. The constructive effects of noise on nonlinear systems are widely acknowledged. Indeed, it was discovered that noise can induce a wide range of complex phenomena in neuron models: coherence resonance [1, 2, 3], stochastic resonance [4, 5], noise-induced bursting [6, 7, 8], stochastic generation of large-amplitude oscillations [9, 10, 11], noise-induced suppression of firing [12], noise-induced chaos and order [7, 13, 14], stochastic oscillating bistability in the zone of canard limit cycles [15], noise-induced transitions between tonic spiking and bursting regimes [16].

In this paper, on the base of the three-dimensional Hindmarsh–Rose model [17, 18, 19], we study a new phenomenon observed in neuron systems: the noise-induced torus bursting. We show that in the parametric zone close to the Neimark–Sacker bifurcation, where the Hindmarsh–Rose system exhibits the rapid spiking oscillations, random disturbances can transform the spiking regime to the torus bursting one. For the quantitative analysis of this phenomenon, we suggest and apply an approach based on the stochastic sensitivity function technique and confidence domains [20, 21, 12].

The present paper is organized as follows. Section 2 discusses the essential features of the the deterministic dynamics of the Hindmarsh–Rose model in the parametric zone of quasi-periodic oscillations. In section 3, we describe the phenomenon of noise-induced torus bursting by direct numerical simulations of solutions of the stochastic Hindmarsh–Rose model. The probabilistic distribution of random trajectories under variation of noise intensity as well as the interspike intervals statistics are studied. In section 4, we suggest and apply the method of analysis of this phenomenon based on the stochastic sensitivity function technique.

Copyright © by the paper's authors. Copying permitted for private and academic purposes.

In: A.A. Makhnev, S.F. Pravdin (eds.): Proceedings of the International Youth School-conference «SoProMat-2017», Yekaterinburg, Russia, 06-Feb-2017, published at <http://ceur-ws.org>

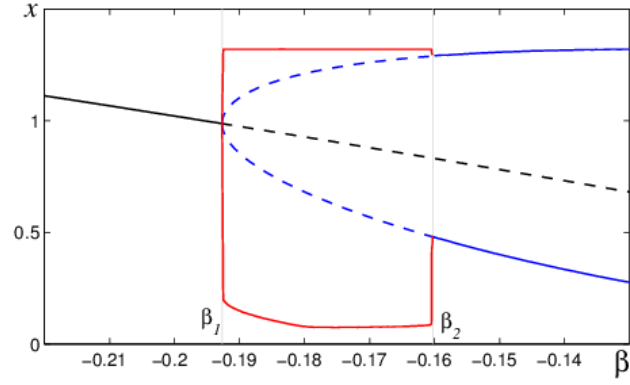


Figure 1: Bifurcation diagram: stable (black solid) and unstable (black dashed) equilibria, maximal and minimal values of x coordinates along stable (blue solid) and unstable (blue dashed) limit cycles, maximal and minimal values of x coordinates along invariant tori (red solid).

2 Deterministic system

Consider the following variant [18] of the Hindmarsh-Rose (HR) model [17]:

$$\begin{aligned}\dot{x} &= sax^3 - sx^2 - y - bz \\ \dot{y} &= \varphi(x^2 - y) \\ \dot{z} &= r(s\alpha x + \beta - kz),\end{aligned}\tag{1}$$

where x is a membrane potential, y is a gating variable, z is a recovery variable; $a, b, k, r, s, \alpha, \beta, \varphi$ are the parameters of the system. The small parameter r ($0 < r \ll 1$) controls the separation of time scales.

Following [19], we fix $a = 0.5, b = 10, k = 0.2, s = -1.95, \alpha = -0.1, \varphi = 1, r = 10^{-5}$.

Consider the dynamics of the system (1) under variation of the parameter β .

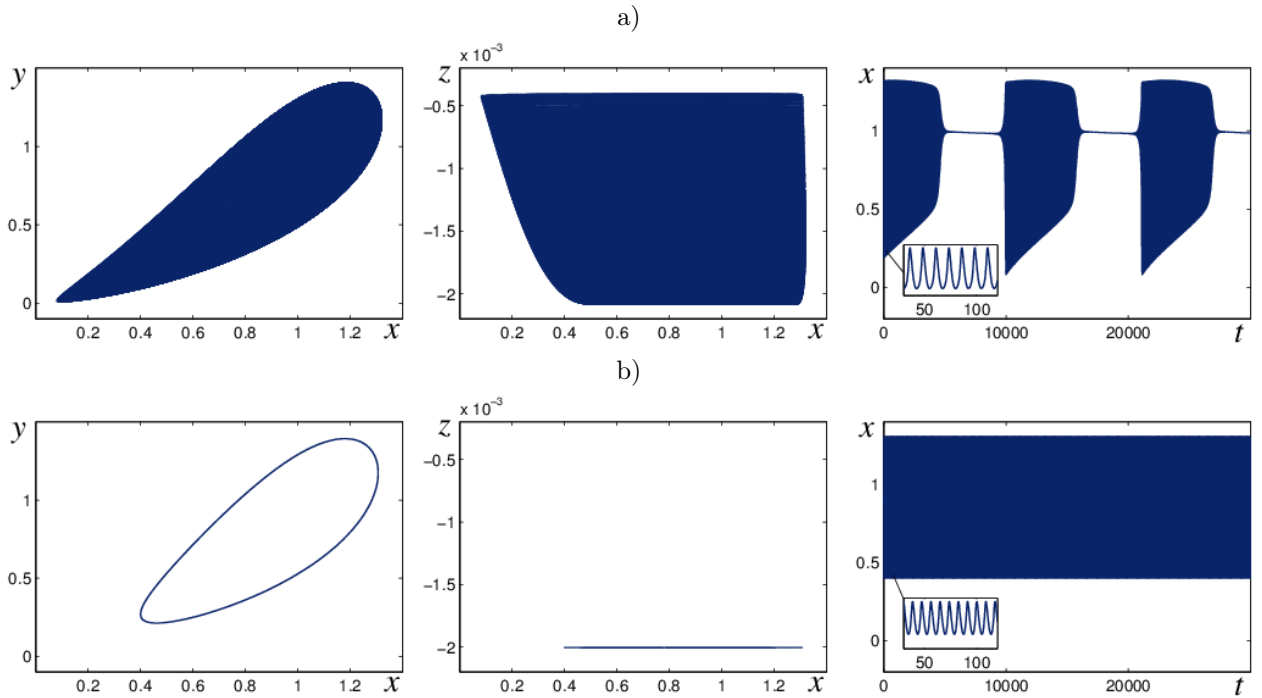


Figure 2: Deterministic trajectories (in projection on xOy, xOz planes) and corresponding time series $x(t)$ for a) $\beta = -0.162$, b) $\beta = -0.15$.

Fig. 1 shows the bifurcation diagram of the deterministic system (1) in the zone $\beta \in (-0.22, -0.13)$. For $\beta < \beta_1 \approx -0.1927$, the system possesses a stable equilibrium. As β increases, the equilibrium loses stability via the supercritical Andronov–Hopf bifurcation at $\beta = \beta_1$, resulting in the emergence of a stable limit cycle. The limit cycle remains stable in a very narrow parameter region: near the Andronov–Hopf bifurcation, the Neimark-Sacker bifurcation with a generation of an invariant torus occurs. Stable tori exist in the system for $-0.1927 \lesssim \beta < \beta_2 \approx -0.1603$. As the parameter passes the point $\beta = \beta_2$, the second Neimark-Sacker bifurcation occurs, and for $\beta > \beta_2$ the stable limit cycle becomes the only attractor. The transition from the limit cycles to the tori near the bifurcation point $\beta = \beta_2$ is accompanied with the torus canard explosion [19].

The tori in the zone $\beta_1 < \beta < \beta_2$ of the model (1) describe a special type of bursting oscillations. The limit cycles in the zone $\beta > \beta_2$ reproduce the rapid tonic spiking behavior. The examples of these two dynamic regimes are shown in Fig. 2 for $\beta = -0.162$ (torus attractor; bursting regime) and $\beta = -0.15$ (limit cycle attractor; tonic spiking regime). In the case of torus bursting, one can observe an alternation of intervals of rapid spiking with long quiescent phases (see Fig. 2a), whereas in the tonic spiking regime, spikes are generated continuously (see Fig. 2b).

3 Noise-induced transition from tonic spiking to torus bursting

Consider the stochastic variant of the model (1):

$$\begin{aligned}\dot{x} &= sax^3 - sx^2 - y - bz + \varepsilon\dot{w}, \\ \dot{y} &= \varphi(x^2 - y) \\ \dot{z} &= r(s\alpha x + \beta - kz),\end{aligned}\tag{2}$$

here w is a standard Wiener process with $E(w(t) - w(s)) = 0$, $E(w(t) - w(s))^2 = |t - s|$, and the value ε is a noise intensity.

Here, we focus on the parametric zone $\beta > \beta_2 \approx -0.1603$, where the unforced deterministic system (1) exhibits the tonic spiking oscillations. For the numerical simulation of random trajectories, the standard Runge–Kutta fourth-order deterministic scheme with corresponding stochastic terms and the time step 0.0001 was used.

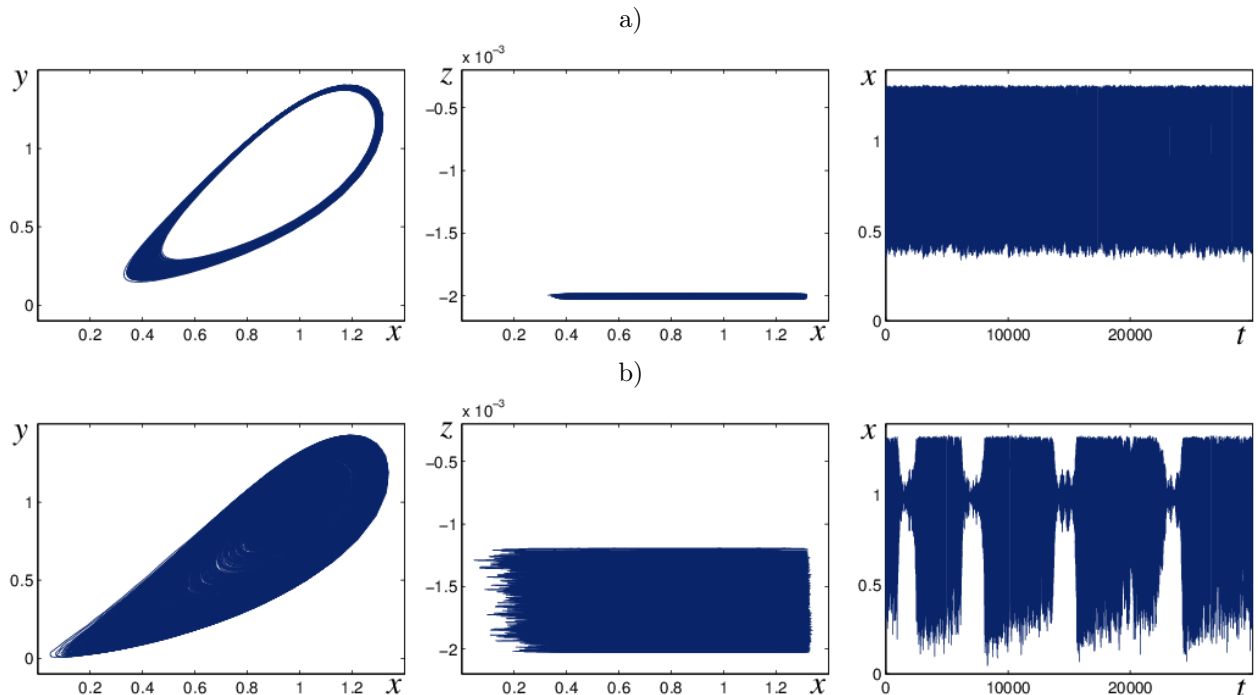


Figure 3: Stochastic trajectories (in projection on xOy , xOz planes) and corresponding time series $x(t)$ for $\beta = -0.15$: a) $\varepsilon = 0.001$, b) $\varepsilon = 0.005$.

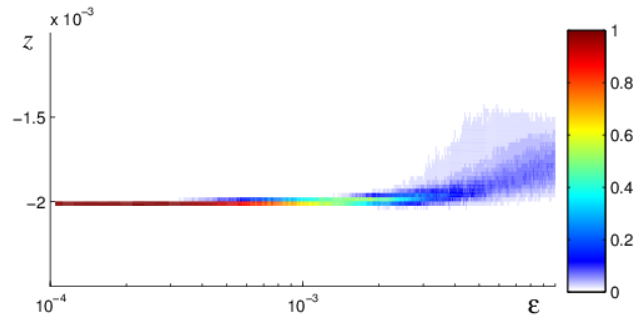


Figure 4: Noise-induced torus bursting: changes of the probability density distribution of z -coordinates of stochastic trajectories for $\beta = -0.15$ in dependence on noise intensity.

Consider the value $\beta = -0.15$. Here, the limit cycle is the attractor of the deterministic system (1). Fig. 3 shows the random trajectories starting from this deterministic cycle and the corresponding time series $x(t)$ for two values of the noise intensity. For a relatively small noise intensity value ($\varepsilon = 0.001$), random trajectories are concentrated in a small vicinity of the deterministic limit cycle, and the type of oscillations remains spiking (see Fig. 3a). For a greater noise intensity ($\varepsilon = 0.005$), random trajectories deviate far from the limit cycle and form a structure similar to a torus (see Fig. 3b). On the $x(t)$ plot, one can observe the alternation of large amplitude spiking oscillations and small amplitude fluctuations near the unstable equilibrium. This indicates that under noise, the type of oscillations changed from tonic spiking to bursting.

Let us study the details of the noise-induced transition from tonic spiking regime to the bursting one by examining the changes of the distribution of random trajectories under increasing noise. Fig. 4 shows the changes of probability density distribution of z -coordinates of stochastic trajectories for $\beta = -0.15$ in dependence on noise intensity. For small noise intensities, random states are localized near the deterministic limit cycle and have a sufficiently small dispersion. With an increase of noise, the dispersion of random states abruptly grows. This corresponds to the emergence of noise-induced torus oscillations.

A probability density distribution of random trajectories can be considered as a spacial characteristic for noise-induced torus bursting. As for an additional temporal (frequency) characteristic, interspike intervals (ISI) statistics can be used.

An estimation of interspike intervals τ distribution is a common method to study stochastic changes in oscillatory dynamics of neuron models. Such statistics of ISIs as the mean value $m = \langle \tau \rangle$, and the coefficient of variation (CV), $C_V = \frac{\sqrt{\langle (\tau - m)^2 \rangle}}{m}$, are widely applied.

Fig. 5 shows the overall mean value m (Fig. 5a) and the overall coefficient of variation C_V (Fig. 5b) of ISIs for different parameter β values under variation of the noise intensity. One can observe that for small noise, the mean ISI is almost constant and corresponds to the period of spiking limit cycle. The increase of the noise intensity causes the abrupt rise of the mean ISI due to the emergence of long ISIs corresponding to the quiescence phase in bursting regime. The plots of overall CV display the anti-coherence (the increase of variability of ISIs

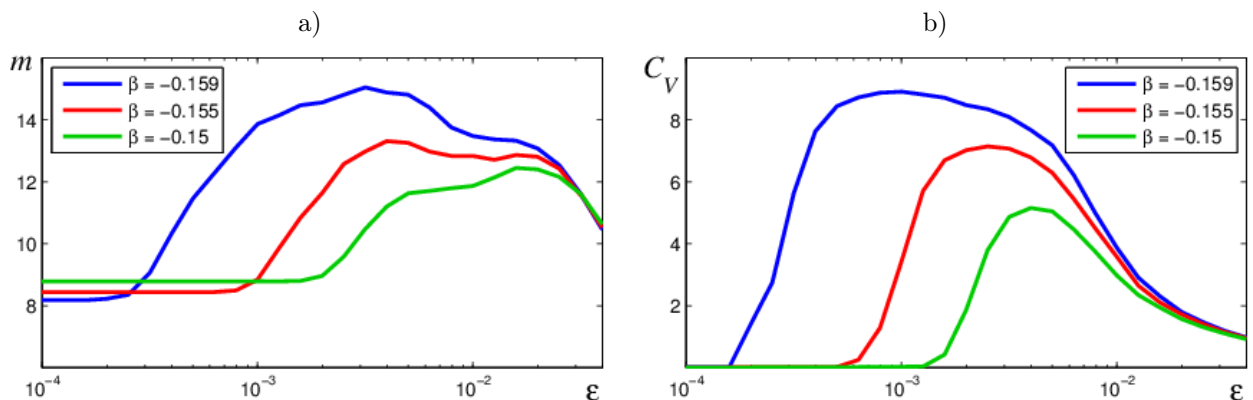


Figure 5: ISI statistics: a) mean value (overall), b) coefficient of variation (overall).

under random disturbances). This is also typical for the bursting dynamics. With the further increase of the noise intensity, the variability of ISIs decreases, which corresponds to the growth of the system coherence.

Thus, in the parametric zone $\beta > \beta_2$, where the limit cycle is the attractor of the deterministic system (1), random disturbances form a new dynamical structure resembling a torus, and the dynamical regime changes from spiking to bursting. Figs. 4 and 5 allow us to make empirical estimations for critical values of noise intensity, corresponding to the transition from the spiking regime to the bursting one. For example, for the considered parameter value $\beta = -0.15$ we get $\varepsilon^* \approx 0.003$. In follows, we show that these critical values of noise intensity can be found analytically.

4 Stochastic sensitivity analysis

The emergence of the torus type stochastic oscillations is related to the peculiarities of the geometrical arrangement of deterministic trajectories near the limit cycle and its stochastic sensitivity.

Fig. 6 shows the deterministic trajectories started from different points in the vicinity of the limit cycle for $\beta = -0.15$. The trajectories tend to the stable cycle, but the character of this movement can be different. One can determine two types of transient regimes in the phase space. In the first type, the trajectory tends to the limit cycle monotonically (see purple color in Fig. 6). In the second type of transient, the trajectory first goes far from the limit cycle, spend a long time in the vicinity of the unstable equilibrium, and then makes a long approach to the cycle (see blue color in Fig. 6). The type of the transient regime depends on the location of the initial point. Thus, there is some border surface between these transient regimes in the phase space. Let us define this border by term ‘‘pseudo-separatrix’’.

The behavior of the system in the presence of random disturbances is also influenced by the stochastic sensitivity of attractors. To conduct the parametric analysis of the noise-induced torus bursting, we apply the stochastic sensitivity function (SSF) technique [20, 21].

Let us consider a general nonlinear system of stochastic differential equations:

$$dx = f(x) dt + \varepsilon \sigma(x) dw(t). \quad (3)$$

Here, x is an n -vector, $f(x)$ is a smooth n -dimensional function, $w(t)$ is n -dimensional standard Wiener process with $E(w(t) - w(s)) = 0$, $E(w(t) - w(s))^2 = |t - s|$, $\sigma(x)$ is an $n \times n$ matrix function, and ε is a scalar parameter of noise intensity.

Let the corresponding deterministic system ($\varepsilon = 0$) have an exponentially stable limit cycle Γ , defined by a T -periodic solution $\bar{x}(t) = \bar{x}(t + T)$.

Let Π_t be a hyperplane that is orthogonal to the cycle at the point $\bar{x}(t)$ ($0 \leq t < T$). For this plane, in the neighborhood of the point $\bar{x}(t)$, a Gaussian approximation of the stationary probabilistic distribution of random

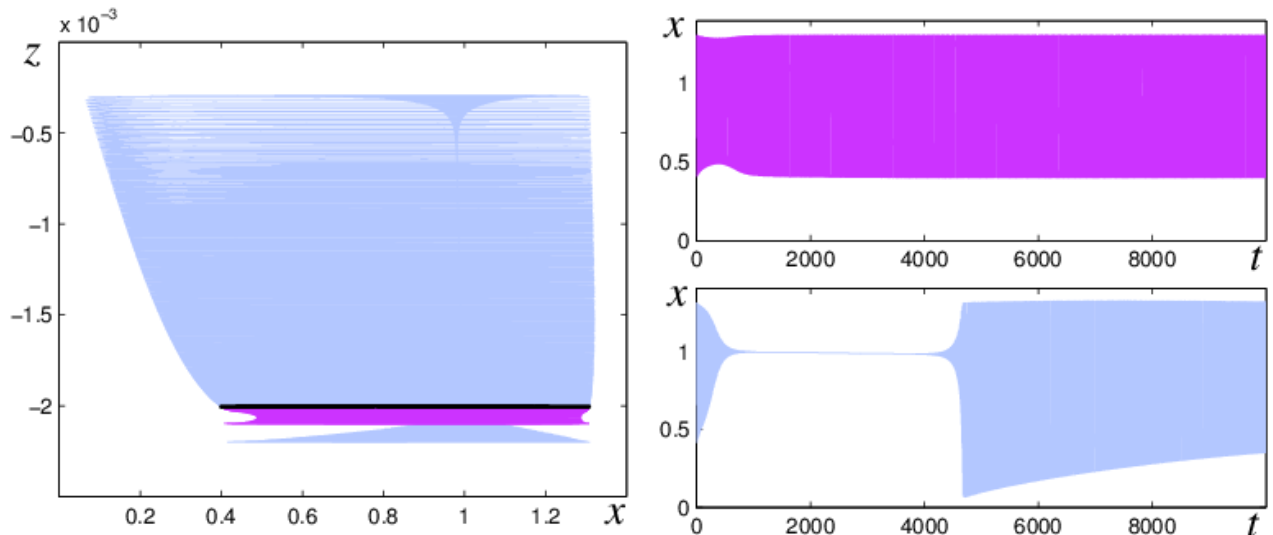


Figure 6: Deterministic limit cycle (black) and phase trajectories (blue and purple) starting from different initial points for $\beta = -0.15$ with corresponding time series $x(t)$.

states can be written [20] as:

$$\rho_t(x, \varepsilon) = K \exp\left(-\frac{(x - \bar{x}(t))^\top W^+(t)(x - \bar{x}(t))}{2\varepsilon^2}\right)$$

with the mean value $m_t = \bar{x}(t)$ and the covariance matrix $D(t, \varepsilon) = \varepsilon^2 W(t)$. Here, the matrix function $W(t)$ is singular ($\det W = 0$), and the sign "+" means a pseudoinversion. The matrix $W(t)$ is a unique solution of the boundary problem

$$\dot{W} = F(t)W + WF^\top(t) + P(t)S(t)P(t) \quad (4)$$

with conditions

$$W(T) = W(0), \quad W(t)r(t) = 0.$$

Here

$$F(t) = \frac{\partial f}{\partial x}(\bar{x}(t)), \quad S(t) = G(t)G^\top(t), \quad G(t) = \sigma(\bar{x}(t)),$$

$$r(t) = f(\bar{x}(t)), \quad P(t) = P_{r(t)}, \quad P_r = I - \frac{rr^\top}{r^\top r}.$$

The stochastic sensitivity function $W(t)$ characterises a sensitivity of a stable limit cycle to noise. In Fig. 7a, the nonzero eigenvalues $\lambda_{1,2}(t)$ of the the matrix function $W(t)$ for $\beta = -0.15$ are plotted. One can observe that the stochastic sensitivity vary nonuniformly along the cycle.

To determine the stochastic sensitivity of the cycle as a whole, the stochastic sensitivity factor $M = \max_{[0, T]} \lambda_1(t)$ can be used. In Fig. 7b, the stochastic sensitivity factor $M(\beta)$ for limit cycles in the zone $\beta \in (-0.1603, -0.14)$ is plotted. One can observe that as the parameter β approaches to the point $\beta = -0.1603$ where the system undergoes the Neimark–Sacker bifurcation, the sensitivity of the limit cycle grows unlimitedly.

The SSF technique allows us to approximate the geometry of bundle of stochastic trajectories around the deterministic limit cycle. Eigenvalues and eigenvectors of the SSF matrix $W(t)$ define a confidence ellipse located in the plane Π_t with the center at the point $\bar{x}(t)$:

$$(x - \bar{x}(t))^\top W^+(t)(x - \bar{x}(t)) = 2q^2\varepsilon^2,$$

where the parameter q determines a fiducial probability $P = 1 - e^{-q}$. With the given probability P , random states belong to the set specified by this confidence ellipse. A set of these ellipses for all points $\bar{x}(t)$ forms in the 3D-space a confidence torus around the limit cycle. Fig. 8a shows the confidence torus (a set of confidence ellipses) around the deterministic limit cycle for $\beta = -0.15$, $\varepsilon = 0.0005$ with fiducial probability $P = 0.99$.

Let us consider the mutual position of the confidence torus and pseudo-separatrix under different noise intensities. Consider the point of the limit cycle from the transition zone (i.e. the part of a limit cycle, from which the transition to the "bursting" zone of phase space occurs more frequently), and the a plane orthogonal to the limit cycle at this point. Let us construct the pseudo-separatrix line, which is an intersection of the pseudo-separatrix surface with the considered plane, and confidence ellipses in this plane. Fig. 8b displays a point of

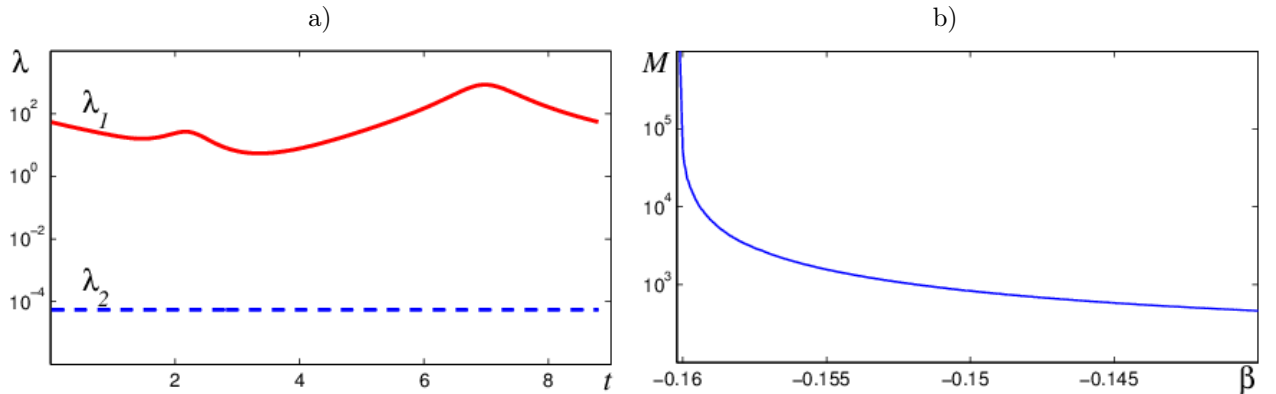


Figure 7: Stochastic sensitivity of limit cycles: a) nonzero eigenvalues $\lambda_{1,2}(t)$ of stochastic sensitivity matrix for $\beta = -0.15$, b) stochastic sensitivity factor $M(\beta)$ in the zone of tonic spiking limit cycles.

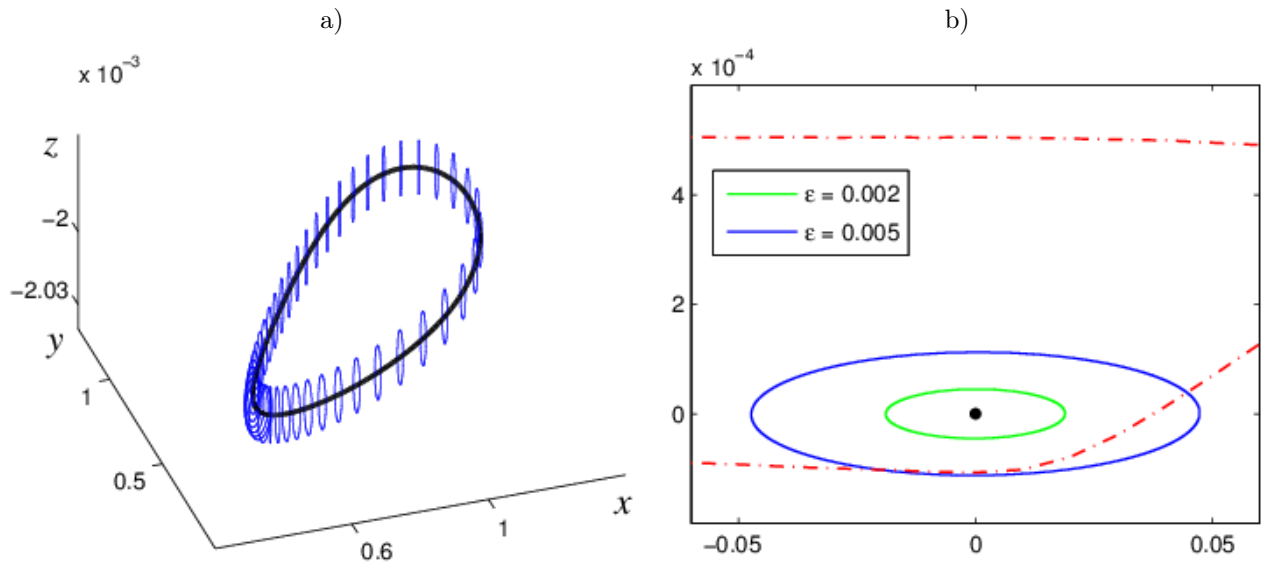


Figure 8: a) Set of confidence ellipses (confidence torus) around the limit cycle for $\beta = -0.15$, $\varepsilon = 0.0005$; b) Point of limit cycle (black circle), confidence ellipses (solid), pseudo-separatrix (dash-dotted) in a normal plane for $\beta = -0.15$; the fiducial probability is $P = 0.99$.

cycle from the transition zone, pseudo-separatrix for $\beta = -0.15$, and the confidence ellipses for different noise intensities. For the sufficiently small noise intensity, a confidence ellipse is close to the deterministic cycle. With an increase of the noise intensity, the ellipse expands and intersects the pseudo-separatrix. Such intersection signals that with high probability, stochastic trajectories can go to the zone of the phase space where they form a stochastic torus. The noise intensity that corresponds to the intersection of the confidence ellipse with pseudo-separatrix can be used as an estimation of the critical value ε^* . For $\beta = -0.15$ we get the value $\varepsilon^* \approx 0.003$ which is in a good agreement with the results of the direct numerical simulations.

5 Conclusion

We studied the stochastic dynamics of the Hindmarsh–Rose model of neuronal activity in the parametrical zone close to the Neimark–Sacker bifurcation of the invariant torus generation. We showed that in this zone, random disturbances transform the tonic spiking dynamic regime into the bursting one. This stochastic phenomenon is confirmed by the approximations of the probability density functions for the distribution of random trajectories as well as the interspike intervals statistics. For a quantitative analysis of the noise-induced bursting, we suggested and applied a constructive approach based on the stochastic sensitivity function technique and the method of confidence domains. This method showed its reliability by a good agreement with the results of the direct numerical simulations.

Acknowledgements

The work was supported by Russian Science Foundation (N 16-11-10098).

References

- [1] A. S. Pikovsky, J. Kurths. Coherence resonance in a noise-driven excitable system. *Phys. Rev. Lett.*, 78:775-778, 1997.
- [2] B. Lindner, L. Schimansky-Geier. Analytical approach to the stochastic FitzHugh–Nagumo system and coherence resonance. *Phys. Rev. E*, 60:7270–7276, 1999.
- [3] B. Lindner, J. Garcia-Ojalvo, A. Neiman, L. Schimansky-Geier. Effects of noise in excitable systems. *Physics Reports*, 392:321-424, 2004.
- [4] A. Longtin. Autonomous stochastic resonance in bursting neurons. *Phys. Rev. E*, 55:868-876, 1997.

- [5] J. Baltanas, J. Casado. Noise-induced resonances in the Hindmarsh–Rose neuronal model. *Phys. Rev. E*, 65:041915, 2002.
- [6] A. B. Neiman, T. A. Yakusheva, D. F. Russell. Noise-induced transition to bursting in responses of paddlefish electroreceptor afferents. *J. Neurophysiol.*, 98:2795–2806, 2007.
- [7] I. Bashkirtseva, S. Fedotov, L. Ryashko, E. Slepukhina. Stochastic Bifurcations and Noise-Induced Chaos in 3D Neuron Model. *International Journal of Bifurcation and Chaos*, 26(12):1630032, 2016.
- [8] L. Ryashko, E. Slepukhina, V. Nasyrova. Noise-induced bursting in Rulkov model. *AIP Conference Proceedings*, 1773:060006, 2016.
- [9] L. B. Ryashko, E. S. Slepukhina. Stochastic generation of bursting oscillations in the three-dimensional Hindmarsh-Rose model. *Journal of Siberian Federal University - Mathematics and Physics*, 9(1):79-89, 2016.
- [10] E. S. Slepukhina. Noise-induced large amplitude oscillations in the Morris-Lecar neuron model with class 1 excitability. *Нелинейная Динамика*, 12(3):327-340, 2016 (in Russian). = E. С. Слепухина. Индуцированные шумом колебания больших амплитуд в модели нейрона Моррис–Лекара с возбудимостью класса 1. *Нелинейная Динамика*, 12(3):327-340, 2016.
- [11] I. Bashkirtseva, L. Ryashko, E. Slepukhina. Analysis of stochastic phenomena in 2D Hindmarsh-Rose neuron model. *AIP Conference Proceedings*, 1773:060003, 2016.
- [12] I. Bashkirtseva, A. B. Neiman, L. Ryashko. Stochastic sensitivity analysis of noise-induced suppression of firing and giant variability of spiking in a Hodgkin-Huxley neuron model. *Phys. Rev. E*, 91:052920, 2015.
- [13] I. Bashkirtseva, L. Ryashko, E. Slepukhina. Order and chaos in the stochastic Hindmarsh-Rose model of the neuron bursting. *Nonlinear Dynamics*, 82(1):919-932, 2015.
- [14] I. Bashkirtseva, S. Fedotov, L. Ryashko, E. Slepukhina. Stochastic dynamics and chaos in the 3D Hindmarsh-Rose model. *AIP Conference Proceedings*, 1790:150007, 2016.
- [15] I. Bashkirtseva, L. Ryashko, E. Slepukhina. Noise-induced oscillation bistability and transition to chaos in FitzHugh-Nagumo model. *Fluctuation and Noise Letters*, 13(1):1450004, 2014.
- [16] L. B. Ryashko, E. S. Slepukhina. Analysis of noise-induced transitions between spiking and bursting regimes in Hindmarsh-Rose neuron model. *CEUR Workshop Proceedings*, 1662:306-314, 2016.
- [17] J.L. Hindmarsh, R.M. Rose. A model of neuronal bursting using three coupled first order differential equations. *Proc. R. Soc. Lond. B Biol. Sci.*, 221:87-102, 1984.
- [18] K. Tsaneva-Atanasova, H. M. Osinga, T. Riess, A. Sherman. Full system bifurcation analysis of endocrine bursting models. *J. Theor. Biol.*, 264(4):1133–1146, 2010.
- [19] J. Burke, M. Desroches, A. M. Barry, T. J. Kaper, M. A. Kramer. A showcase of torus canards in neuronal bursters. *Journal of Mathematical Neuroscience*, 2(1):1–46, 2012.
- [20] I. A. Bashkirtseva, L. B. Ryashko. Stochastic sensitivity of 3D-cycles. *Mathematics and Computers in Simulation*, 66:55–67, 2004.
- [21] L. Ryashko, I. Bashkirtseva, A. Gubkin, P. Stikhin. Confidence tori in the analysis of stochastic 3D-cycles. *Mathematics and Computers in Simulation*, 80:256–269, 2009.